ECS | The Electrochemical Society
Advancing solid state & electrochemical science & technology

Effect of Recombination Catalyst Loading in PEMWE Membranes on Anodic Hydrogen Content Reduction

View the article online for updates and enhancements.

Effect of Recombination Catalyst Loading in PEMWE Membranes on Anodic Hydrogen Content Reduction

Dunia Abbas,[1,2,=] Agate Martin,[3,=] Patrick Trinke,[3] Markus Bierling,[1,2]
Boris Bensmann,[3] Simon Thiele,[1,2] Richard Hanke-Rauschenbach,[1] and
Thomas Böhm[1,z]

[1]*Forschungszentrum Jülich GmbH, Helmholtz Institute Erlangen-Nürnberg for Renewable Energy (IEK-11), Cauerstraße 1, 91058 Erlangen, Germany*
[2]*Department of Chemical and Biological Engineering, Friedrich-Alexander-Universität Erlangen-Nürnberg, Egerlandstraße 3, 91058 Erlangen, Germany*
[3]*Leibniz University Hannover, Institute of Electric Power Systems, Appelstraße 9a, 30167 Hannover, Germany*

Integrating platinum-based recombination catalysts into proton exchange membrane water electrolysis systems effectively reduces the anodic hydrogen content. We studied the effect of the platinum loading of an interlayer close to the anode within the membrane on the anodic hydrogen in oxygen content. For the investigated Pt-loadings between 1 μg_{Pt} cm^{-2} and 140 μg_{Pt} cm^{-2}, the results revealed that for a 110 μm membrane, 7 μg_{Pt} cm^{-2} were sufficient to allow a safe operation at cathode pressures up to 10 bar. A further increase of the Pt-loading did not significantly improve the reduction of the anodic hydrogen in oxygen content.

The production of green hydrogen by proton exchange membrane water electrolysis (PEMWE) marks a significant technological milestone in reducing global CO_2 emissions.[1] A cost- and energy-efficient and safe PEMWE operation must be guaranteed for commercialization. The safe operation of PEM electrolyzers relies on effective gas separation by the membranes to avoid the formation of explosive gas mixtures.[2,3] Reducing the membrane thickness increases the system efficiency but increases the gas crossover between the anode and cathode compartments.[4–6] Platinum-based recombination catalysts, e.g., integrated into the membrane,[7–11] within or on top of the anode,[12,13] in the anode porous transport layer (PTL) or external gas recombiner,[14] were shown as well-working mitigation strategies to reduce the anodic hydrogen content in PEMWE systems.[6] In the recombination reaction, permeating hydrogen recombines with oxygen at the catalyst to water. Integrating the recombination catalyst inside the membrane offers the advantage that the catalyst is protected from high anodic potentials, which might lead to a dissolution or passivation of the Pt-nanoparticles in the long-term operation due to the formation of oxides.[7,8] The catalyst position and its loading must be chosen carefully to achieve high recombination effectiveness at minimal material costs. Recently, we found that a Pt-recombination interlayer works most effectively when incorporated close to the anode within the membrane due to the higher oxygen availability for recombination in this region.[15] In this study, we investigate the effect of the catalyst loading at its ideal position close to the anode in the membrane by varying the loading between 1 μg_{Pt} cm^{-2} and 140 μg_{Pt} cm^{-2} and by studying the resulting anodic hydrogen in oxygen content under various operating conditions.

Materials and Methods

Manufacturing of catalyst-coated membranes.—Catalyst-coated membranes (CCMs) were fabricated by hot pressing (160 °C, 2 MPa, 5 min) the electrodes onto the membranes with the Pt-interlayer close to the anode.

Electrodes with an area of 5 cm^2 were prepared with the same procedure as in Ref. 16. Anodes consisted of Umicore Elyst Ir75 and Nafion D2021 (FuelCellStore) with 1.9 ± 0.1 mg$_{Ir}$ cm^{-2} (I/C = 0.13)

and cathodes of Tanaka TEC10V40E and Nafion D2021 with 0.1 ± 0.04 mg$_{Pt}$ cm^{-2} (I/C = 0.65).

A mixture of 25 wt% Nafion D2021 in 2-propanol was prepared for membrane fabrication via spray coating (Sono-Tek). For the different Pt-interlayers, mixtures of Pt-nanoparticles (Sigma-Aldrich, particle size < 50 nm)/ Nafion D2020 (FuelCellStore)/ 2-propanol were prepared in weight ratios of 0.0045/14.3/100, 0.0224/14.3/100, 0.0447/14.3/100, and 0.4470/14.3/100 and stirred for 48 h. The spraying procedure for membranes with interlayers and the reference without interlayer is described in Ref. 15. The Pt-loadings were determined by the weight gain as 1 μg_{Pt} cm^{-2}, 7 μg_{Pt} cm^{-2}, 14 μg_{Pt} cm^{-2}, and 140 μg_{Pt} cm^{-2} (rounded to single-digit μg cm^{-2} range). The measurement error was kept minimal by weighing the samples immediately after removing them from the spray coater's heating plate (65 °C).

In the following, the CCMs will be referred to as IL_1 (1 μg_{Pt} cm^{-2}), IL_7 (7 μg_{Pt} cm^{-2}), IL_14 (14 μg_{Pt} cm^{-2}), and IL_140 (140 μg_{Pt} cm^{-2}) according to their loading. The reference is referred to as no_IL.

Electrochemical Characterization

The test setup and measurement protocols are described in Ref. 15. In brief, the membrane electrode assembly consisted of a carbon PTL (H23I2, Freudenberg) for the cathode side, the CCMs with or without an interlayer, and a titanium PTL (2GDL40–1.00, Bekaert). The materials were assembled in dry state in a 4 cm^2 cell designed by Fraunhofer ISE.[15,17,18]

After thermal equilibration in the cell, a compression force of 3 kN was applied. The crossover measurements were performed at three pressure combinations (p^c = 1 bar and p^a = 1 bar, p^c = 10 bar and p^a = 1 bar, p^c = 10 bar and p^a = 5 bar).

Crossover measurements and performance testing were conducted in an E100 test station (Greenlight Innovation) at 80 °C and 80 ml min^{-1} anode water recirculation with an electrical resistivity of min. 3 MΩ cm. A BCS815 potentiostat (BioLogic) was used as current source. The anode product gas was diluted with a constant oxygen mass flow of 0.04 g min^{-1} (mass flow controller EL-FLOW Prestige, Bronkhorst) directly behind the anode cell outlet to prevent the formation of explosive gas mixtures. The dried gas mixture was supplied to a gas chromatograph (490 μGC System, Agilent, with N_2 as carrier gas) to analyze the anodic hydrogen content during electrolysis operation.

=Equal contribution.
zE-mail: t.boehm@fz-juelich.de

Cross-sectional imaging.—Cross-sections of post-mortem CCMs were prepared by embedding the samples in epoxy resin and subsequent grinding and polishing or ultramicrotomy. Before imaging with a backscattered electron detector by scanning electron microscopy (SEM), the samples were sputter-coated with Au. The membrane thicknesses were evaluated by applying an in-house Matlab script.

Results and Discussion

Cross-sections.—Figure 1a shows the CCM cross-section of IL_140, and Figs. 1b–1e) show magnified sections of the Pt-interlayers with different loadings. The interlayers were positioned close to the anode at a distance of around 10 μm and had a thickness of approximately 8 μm. As expected, the density of the Pt-nanoparticles inside the interlayer increased with increasing loading. The average thickness of the membranes was determined based on the cross-sections as 111 ± 4.5 μm (mean ± standard deviation).
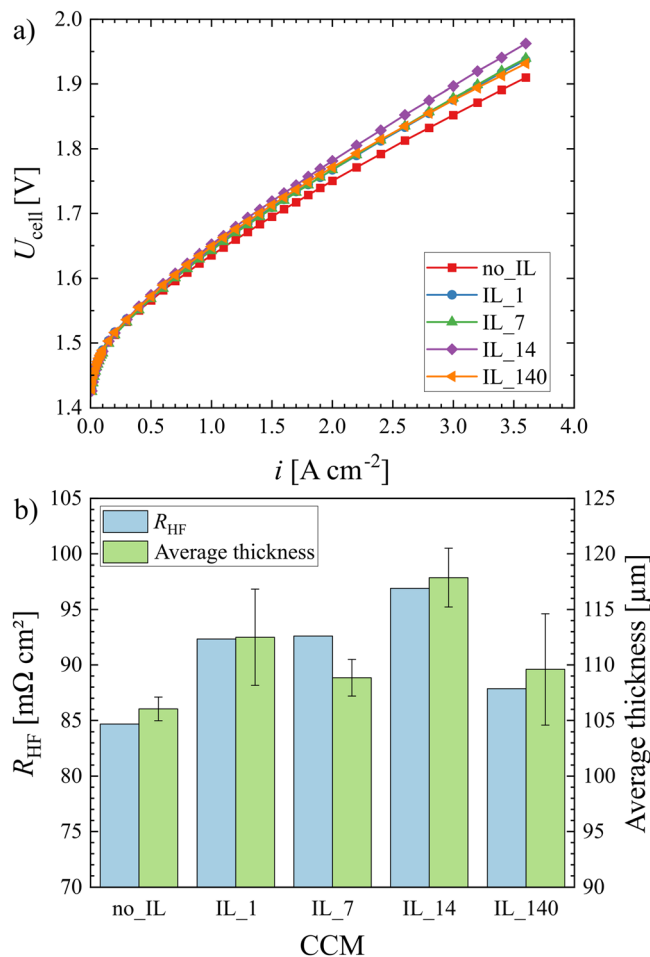
Polarization behavior.—Figure 2a shows the polarization curves recorded at ambient pressure and 80 °C. The CCMs showed a similar kinetic behavior at low current densities with Tafel slopes of 53.58 ±

0.52 mV (mean ± standard deviation). In this region, no clear trend between the Pt-loading of the recombination interlayer and the electrochemical performance could be identified. However, performance deviations between the CCMs were observed above 1 A cm^{-2}. At 3.6 A cm^{-2}, the voltage reached 1.94 ± 0.02 V, with no_IL showing the best and IL_14 the worst performance. For IL_1, IL_7, and IL_140, a similar performance of around 1.94 V at 3.6 A cm^{-2} was measured. The comparable performance of IL_1 and IL_140, despite the significantly higher Pt-loading of the latter, suggests that the Pt-loading does not affect the electrochemical performance. This finding is in good agreement with previous studies.[8,9,15]

The high-frequency resistance (R_{HF}) was analyzed and compared with the membrane thicknesses of each CCM (Fig. 2b) to elucidate the deviations between the CCMs. no_IL had the lowest thickness with 106.04 ± 1.07 μm and the lowest R_{HF} of 84.7 mΩ cm^2, which explains the superior performance of no_IL at increasing current densities. Conversely, IL_14 had an average thickness of 117.87 ± 2.64 μm and the highest R_{HF} of 96.9 mΩ cm^2. The variations of the R_{HF} values and the thicknesses provide insight into the manufacturing tolerances of spray-coated membranes, although they do not
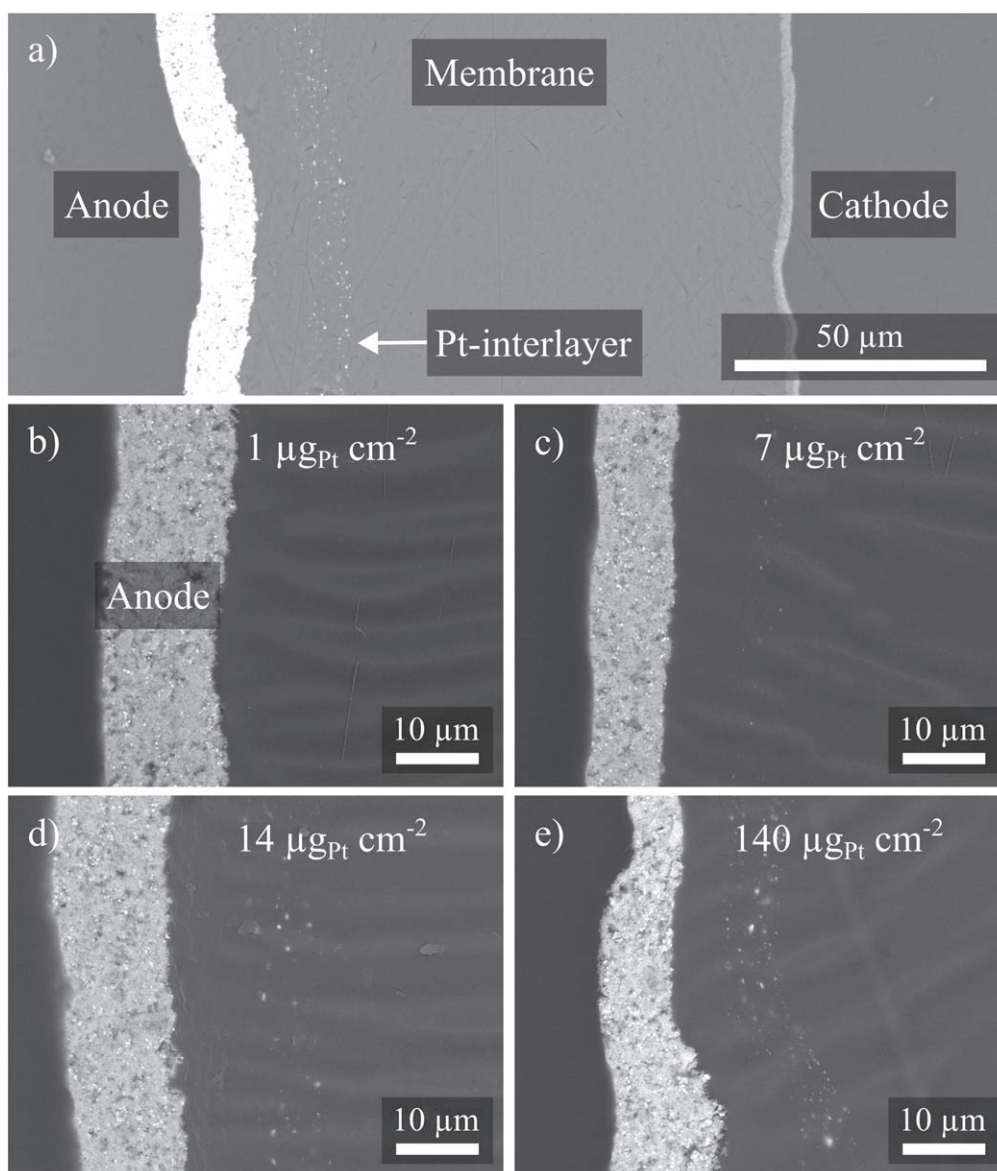


Figure 1. SEM images showing (a) cross-section of IL_140 and magnified sections of the Pt-interlayers of (b) IL_1, (c) IL_7, (d) IL_14, and (e) IL_140 after electrochemical testing.

Figure 2. (a) Polarization behavior and (b) correlation between high-frequency resistance R_{HF} and average membrane thickness.

Figure 3. Anodic hydrogen contents at (a) ambient pressure and (b) $p^c = 10$ bar and $p^a = 1$ bar (filled symbols), and $p^a = 5$ bar (hollow symbols).

correlate perfectly. Therefore, we conclude that the differences in performance originate from manufacturing, assembly, and measurement tolerances and are not related to the investigated Pt-interlayer loadings.

Hydrogen in oxygen content.—Recently, it was found that a Pt-recombination interlayer within the membrane results in the lowest anodic hydrogen content at asymmetric pressure conditions when placed close to the anode.[15] In the mentioned study, the loading of the interlayer was 10 μg_{Pt} cm^{-2}. Thus, the Pt-loading was varied in the present work between three orders of magnitude from 1 μg_{Pt} cm^{-2} to 140 μg_{Pt} cm^{-2} to identify the optimal loading and, consequently, minimize the costs for the interlayer. A maximum content of 2 vol% H$_2$ in O$_2$ (50% of lower explosion limit[5]) is typically regarded as the technical safety limit for the safe operation of PEMWE systems. Therefore, the anodic hydrogen content can be used to evaluate CCMs concerning safety. Figure 3a shows the anodic hydrogen content of the PEMWE cells operated at atmospheric pressure. For all CCMs, the hydrogen content was below the safety limit. It was found that the hydrogen content showed a minimum at around 1 A cm^{-2}. This behavior was already reported and explained by the supersaturation of water with evolved hydrogen due to mass transport limitations that lead to insufficient removal of hydrogen.[17] As expected, the anodic hydrogen content was the highest with no_IL and decreased with increasing Pt-loading. With the lowest Pt-loading of 1 μg_{Pt} cm^{-2} (IL_1), a reduction of the hydrogen content by up to 50% was achieved (e.g., 0.13 vol% to 0.06 vol% at 0.5 A cm^{-2}). For IL_7, the hydrogen content reached around 0.02 vol%, corresponding to a reduction of around 85%
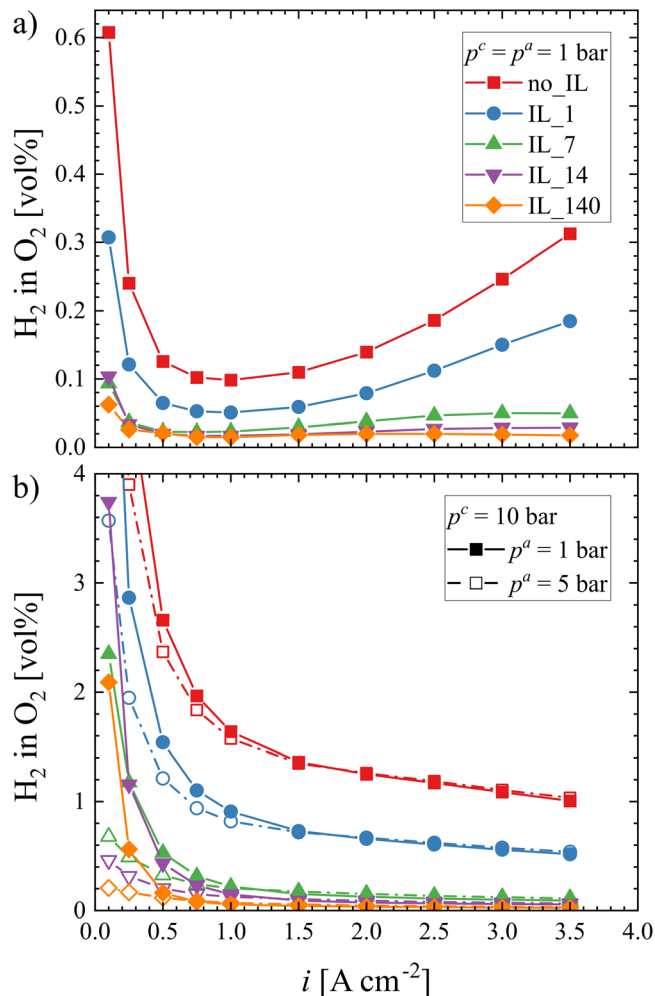
compared to no_IL. Increasing the loading above 7 μg_{Pt} cm^{-2} did not lead to a significant further reduction.

The differential pressure operation of PEMWEs is desirable in industrially relevant applications. However, it is also most safety-critical in terms of hydrogen crossover rates.[10,14] Increasing the cathode pressure increases the hydrogen concentration in the cathode catalyst layer, which leads to an increased driving force for hydrogen crossover via the solution-diffusion mechanism.[4,17,19]

Therefore, the anodic hydrogen content measured at $p^c = 10$ bar and $p^a = 1$ bar was higher than at ambient pressure conditions (filled symbols, Fig. 3b). The anodic hydrogen content decreased significantly when adding a Pt-interlayer. While for no_IL, a safe operation (H$_2$ in O$_2$ < 2 vol%) was only ensured for current densities above 1 A cm^{-2}, the operational window included 0.5 A cm^{-2} for IL_1. For IL_7, IL_14, and IL_140, the system could be safely operated down to 0.25 A cm^{-2}.

For an effective recombination, hydrogen and oxygen must simultaneously be available at the recombination catalyst. Due to the lower production rate and permeability of oxygen compared to hydrogen, the oxygen concentration in the membrane represents a limiting factor for recombination.[20–22] A similar finding was made for PEM fuel cells. It was shown that dissolved Pt-particles from the oxygen side migrate into the membrane and form a Pt-band close to this electrode. At this position, the permeating gases are completely recombined at the Pt-catalyst.[23] Hence, one way to further increase the operational window is to increase the pressure and, thus, the oxygen concentration at the anode, as was shown in our previous study.[15] This observation was confirmed by measuring the anodic
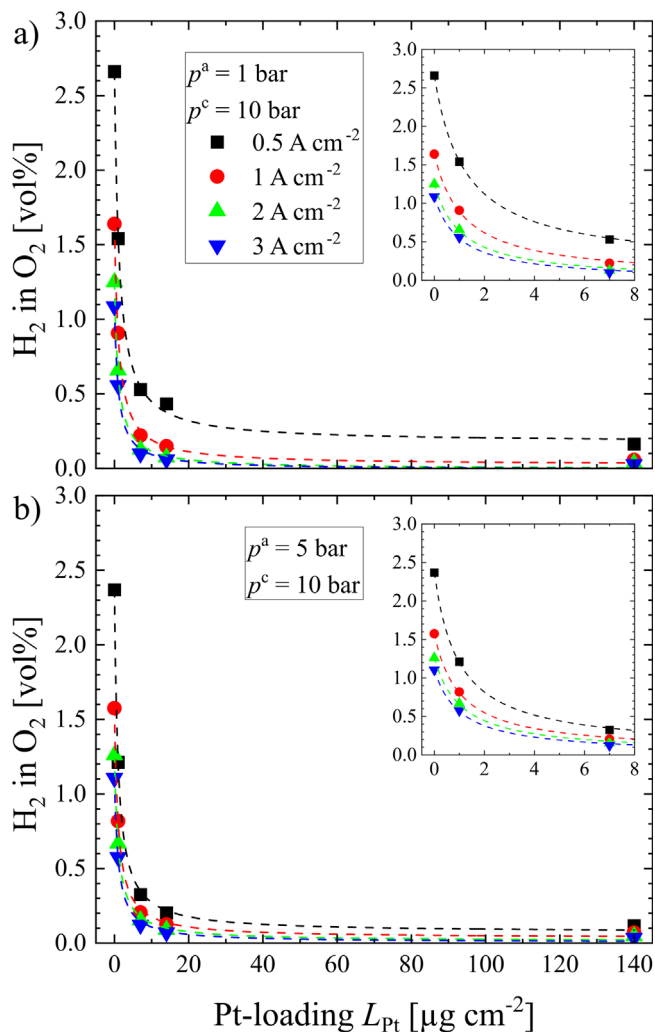
Figure 4. Anodic hydrogen content as a function of the Pt-loading measured at $p^c = 10$ bar and (a) $p^a = 1$ bar and (b) $p^a = 5$ bar for different current densities. The data were fitted with H_2 in $O_2 = \frac{a}{1 + b \times L_{Pt}} + c$ (dashed lines, $R^2 > 0.99$ for all data sets).

hydrogen content at $p^c = 10$ bar and $p^a = 5$ bar (hollow symbols, Fig. 3b). The oxygen concentration within the membrane increases by increasing the anode pressure to 5 bar. Thus the recombination effectiveness improved, e.g., for IL_7 the anodic hydrogen content was reduced from 2.35 vol% to 0.68 vol% at 0.1 A cm^{-2}. Hence, the operational window was further increased, and the PEMWE system could be operated in the complete current density range without safety concerns for loadings of 7 µg$_{Pt}$ cm^{-2} and above. However, a further reduction of the anodic hydrogen content with increasing anode pressure was only observed for current densities up to 1 A cm^{-2}. At higher current densities, the anodic hydrogen contents were similar for the two investigated anode pressures.

This finding suggests that the oxygen concentration at the recombination interlayer at higher current densities seems to be no longer limiting. One possible explanation could be that the oxygen crossover through the membrane increases stronger with current density than the hydrogen crossover. Hence, at higher current densities, enough oxygen would be available. However, at the moment, it is not possible to measure the oxygen crossover during PEMWE operation, and consequently, this assumption cannot be confirmed.

In order to establish a reasonable trade-off between the recombination effectiveness and the required Pt-loading, we investigated the anodic hydrogen content as a function of the Pt-loading for different current densities and operating pressures.

The crossover reduction for other Pt-loadings was estimated by interpolating the anodic hydrogen contents measured at $p^c = 10$ bar and $p^a = 1$ bar (Fig. 4a), and $p^a = 5$ bar (Fig. 4b). In both cases, the anodic hydrogen content asymptotically approached a current density-dependent minimum value with increasing Pt-loading. For instance, at 0.5 A cm^{-2} and $p^a = 1$ bar, the hydrogen content was reduced by 42% for IL_1 and 80% for IL_7 compared to no_IL. By further increasing the loading from IL_7 to IL_14, the anodic hydrogen content was only reduced by an additional 0.1 vol%. At the highest investigated loading of 140 µg$_{Pt}$ cm^{-2}, the anodic hydrogen content remained around 0.16 vol%. At higher current densities, the anodic hydrogen content approached values close to zero for Pt-loadings above 7 µg$_{Pt}$ cm^{-2}.

Increasing the anode pressure (Fig. 4b) reduced the asymptotic minimum value at 0.5 A cm^{-2} by 28%. These results imply a limitation in oxygen availability at low current densities and low anodic pressures, even at higher Pt-loadings. Consequently, a further increase of the Pt-loading cannot reduce the hydrogen in oxygen content.

Conclusions

The impact of Pt-recombination interlayer loadings between 1 µg$_{Pt}$ cm^{-2} and 140 µg$_{Pt}$ cm^{-2} on the resulting anodic hydrogen content in PEMWE cells was investigated. It was found that the different Pt-loadings in the CCMs extended the operational window of PEMWEs without impairing the electrochemical performance. For the investigated experimental case, a Pt-interlayer close to the anode at a loading of around 10 µg$_{Pt}$ cm^{-2} is an ideal compromise between low material costs and effective prevention of explosive gas mixtures at the anode. However, it has to be noted that the precise loading needs to be evaluated depending on the desired operating parameters and CCM properties, e.g., the equivalent weight of the membrane, membrane thickness, Pt-interlayer position, and recombination catalyst particle size.

A previous study has proven long-term stability up to 5000 h for a recombination interlayer.[11] However, the effect of loading reduction on stability remains to be elucidated. Further, it is important for the efficiency of the recombination catalyst to identify not only the ideal position and loading but also the optimal particle size. Particle size influences the recombination effectiveness for a given Pt-loading since the surface area increases with decreasing particle sizes. We could show that very low Pt-loadings significantly reduce the anodic hydrogen content in PEMWE cells. Based on the findings about the ideal position[15] and loading of the Pt-interlayer, we aim to develop a comprehensive theoretical model of the recombination mechanism, where the impact of different operating conditions and the related oxygen availability is evaluated for different membrane thicknesses and interlayer configurations.

ORCID

Dunia Abbas https://orcid.org/0000-0002-3938-0026
Agate Martin https://orcid.org/0000-0003-4673-1135
Patrick Trinke https://orcid.org/0000-0002-0935-5321
Markus Bierling https://orcid.org/0000-0002-4992-2095
Boris Bensmann https://orcid.org/0000-0001-8685-7192
Simon Thiele https://orcid.org/0000-0002-4248-2752
Richard Hanke-Rauschenbach https://orcid.org/0000-0002-1958-307X
Thomas Böhm https://orcid.org/0000-0003-2036-2159

References

1. S. Shiva Kumar and V. Himabindu, *Materials Science for Energy Technologies*, **2**, 442 (2019).
2. C. van Pham, D. Escalera-López, K. Mayrhofer, S. Cherevko, and S. Thiele, *Adv. Energy Mater.*, **11**, 2101998 (2021).
3. U. Babic, M. Suermann, F. N. Büchi, L. Gubler, and T. J. Schmidt, *J. Electrochem. Soc.*, **164**, F387 (2017).
4. M. Schalenbach, M. Carmo, D. L. Fritz, J. Mergel, and D. Stolten, *Int. J. Hydrog. Energy*, **38**, 14921 (2013).
5. H. Janssen, J. C. Bringmann, B. Emonts, and V. Schroeder, *Int. J. Hydrog. Energy*, **29**, 759 (2004).
6. P. Trinke, P. Haug, J. Brauns, B. Bensmann, R. Hanke-Rauschenbach, and T. Turek, *J. Electrochem. Soc.*, **165**, F502 (2018).
7. C. Klose, P. Trinke, T. Böhm, B. Bensmann, S. Vierrath, R. Hanke-Rauschenbach, and S. Thiele, *J. Electrochem. Soc.*, **165**, F1271 (2018).
8. A. Stähler, M. Stähler, F. Scheepers, W. Lehnert, and M. Carmo, *J. Electrochem. Soc.*, **169**, 34522 (2022).
9. S. Garbe, E. Samulesson, T. J. Schmidt, and L. Gubler, *J. Electrochem. Soc.*, **168**, 104502 (2021).
10. M. Schalenbach and D. Stolten, *Electrochim. Acta*, **156**, 321 (2015).
11. Z. Zeng et al., *J. Electrochem. Soc.*, **169**, 54536 (2022).
12. N. Briguglio, F. Pantò, S. Siracusano, and A. S. Aricò, *Electrochim. Acta*, **344**, 136153 (2020).
13. N. Briguglio, S. Siracusano, G. Bonura, D. Sebastián, and A. S. Aricò, *Appl. Catal. B*, **246**, 254 (2019).
14. S. A. Grigoriev, P. Millet, S. V. Korobtsev, V. I. Porembskiy, M. Pepic, C. Etievant, C. Puyenchet, and V. N. Fateev, *Int. J. Hydrog. Energy*, **34**, 5986 (2009).
15. A. Martin, D. Abbas, P. Trinke, T. Böhm, M. Bierling, B. Bensmann, S. Thiele, and R. Hanke-Rauschenbach, *J. Electrochem. Soc.*, **168**, 94509 (2021).
16. M. Bernt, A. Siebel, and H. A. Gasteiger, *J. Electrochem. Soc.*, **165**, F305 (2018).
17. A. Martin, P. Trinke, M. Stähler, A. Stähler, F. Scheepers, B. Bensmann, M. Carmo, W. Lehnert, and R. Hanke-Rauschenbach, *J. Electrochem. Soc.*, **169**, 14502 (2022).
18. Fraunhofer Institute for Solar Energy Systems ISE, *Fraunhofer ISE—Annual Report 2020/2021, Freiburg, Germany (2021)*.
19. D. Bessarabov and P. Millet, *in PEM Water Electrolysis* (Amsterdam), (Elsevier) p. 117 (2018).
20. H. Ito, T. Maeda, A. Nakano, and H. Takenaka, *Int. J. Hydrog. Energy*, **36**, 10527 (2011).
21. S. A. Grigoriev, P. Millet, S. V. Korobtsev, V. I. Porembskiy, M. Pepic, C. Etievant, C. Puyenchet, and V. N. Fateev, *Int. J. Hydrogen Energy*, **34**, 5986 (2009).
22. T. Sakai, H. Takenaka, N. Wakabayashi, Y. Kawami, and E. Torikai, *J. Electrochem. Soc.*, **132**, 1328 (1985).
23. H. Wang, X.-Z. Yuan, and H. Li, *PEM Fuel Cell Diagnostic Tools* (Boca Raton, FL), (CRC Press) (2012).